

The Subaru Ly-alpha blob survey: A sample of 100 kpc Ly-alpha blobs at z = 3

Yuichi Matsuda (Durham University, UK)

T. Yamada, T. Hayashino, R. Yamauchi, Y. Nakamura, N. Morimoto, K. Kousai, E. Nakamura, M. Horie, T. Fujii (Tohoku),
M. Ouchi, Y. Ono (Tokyo), M. Umemura & M. Mori (Tsukuba)

ABSTRACT: We present results of a survey for giant Ly-alpha nebulae (LABs) at z=3 with Subaru/Suprime-Cam. We obtained Ly-alpha imaging at z=3.09±0.03 around the SSA22 protocluster and in several blank fields. The total survey area is 2.1 square degrees, corresponding to a comoving volume of 1.6×10^{16} Mpc³. Using a uniform detection threshold of 1.4×10^{-18} erg s⁻¹ cm⁻² arcsec⁻² for the Ly-alpha images, we construct a sample of 14 LAB candidates with major-axis diameters larger than 100 kpc, including 5 previously known blobs and two known quasars. This survey triples the number of known LABs over 100 kpc. The giant LAB sample shows a possible "morphology-density relation": filamentary LABs reside in average density environments as derived from compact Ly-alpha emitters, while circular LABs reside in both average density and over-dense environments. Although it is hard to examine the formation mechanisms of LABs only from the Ly-alpha morphologies, more filamentary LABs may relate to cold gas accretion from the surrounding inter-galactic medium (IGM) and more circular LABs may relate to large-scale gas outflows, which are driven by intense starbursts and/or by AGN activities. Our survey highlights the potential usefulness of giant LABs to investigate the interactions between galaxies and the surrounding IGM from the field to overdense environments at high-redshift.

Table 1. Summary of narrow-band observations

Field	RA (J2000)	Dec (J2000)	Date (mm/yyyy) ^a	Exposure (hours)	Area (arcmin ²)	FWHM (arcsec)	Depth (ABmag) ^b
SXDS-C	02:18:00.0	-05:00:00	08, 09, 10/2005	5.2	682	1.0	0.81
SXDS-N	02:18:00.0	-04:35:00	10/2005	4.8	740	1.0	0.94
SXDS-S	02:18:00.0	-05:25:00	08, 10/2005	4.8	737	1.0	0.82
GOODS-N	12:37:23.6	+02:13:31	04/2005	10.0	869	1.1	0.69
SDF	13:24:39.0	+27:29:26	04/2004, 04/2005	7.2	805	1.0	0.67
SSA22-Sb1	22:17:34.0	+00:17:01	09/2002	7.2	633	1.0	0.92
SSA22-Sb2	22:16:36.7	+00:36:52	08/2004	5.5	487	1.0	0.96
SSA22-Sb3	22:18:36.3	+00:36:52	08, 09/2005	5.5	537	1.0	0.89
SSA22-Sb4	22:19:40.0	+00:17:00	08, 09, 10/2005	5.5	529	1.1	1.15
SSA22-Sb5	22:15:28.0	+00:17:00	09/2005	5.5	565	1.0	1.06
SSA22-Sb6	22:14:30.7	+00:33:52	10/2005	5.5	572	1.0	0.92
SSA22-Sb7	22:17:42.7	+00:56:52	09, 10/2005	5.5	480	1.0	1.02

^aThe 1-σ surface brightness limit (10^{-18} erg s⁻¹ cm⁻² arcsec⁻²).
^bThe 5-σ limiting magnitude calculated with 2 arcsec diameter aperture photometry.

Table 2. Properties of the 14 giant LAB candidates

ID	RA (J2000)	Dec (J2000)	a ^a (kpc)	Area (arcsec ²)	L _{Lyα} (10 ⁴³ erg s ⁻¹)	F ^b	δ _{LAE}	z _{spec}	Note
SSA22-Sb1-LAB1	22:17:25.95	+00:12:37.7	175	181 ± 14	8.1 ± 0.6	0.56	2.7	3.099 ^c	Spm ^d /submm ^e
SSA22-Sb6-LAB1	22:13:48.30	+00:31:32.8	166	116 ± 9	5.8 ± 0.4	0.69	0.6	3.091 ^f	—
SSA22-Sb1-LAB2	22:17:38.99	+00:13:27.8	157	137 ± 8	6.8 ± 0.3	0.59	3.7	3.091 ^f	X-ray ^g /Spm ^d
SSA22-Sb5-LAB1	22:15:33.56	+00:25:16.9	147	59 ± 7	8.8 ± 0.4	0.80	-0.5	—	—
SSA22-Sb3-LAB1	22:17:59.45	+00:30:55.7	126	102 ± 8	20.4 ± 0.3	0.52	1.2	3.099 ^h	QSO ⁱ /Radio ^j
GOODS-N-LAB1	12:35:57.54	+02:10:24.9	124	47 ± 7	5.4 ± 0.5	0.77	0.9	3.075 ^k	QSO ^l /X-ray ^m
SSA22-Sb2-LAB1	22:16:58.37	+00:34:52.0	121	60 ± 15	2.0 ± 0.6	0.70	1.2	—	—
SSA22-Sb2-LAB2	22:16:56.40	+00:27:53.3	115	48 ± 11	1.4 ± 0.2	0.73	-0.1	—	—
SSA22-Sb1-LAB5	22:17:11.66	+00:16:44.4	110	43 ± 11	1.3 ± 0.3	0.74	1.0	—	Spm ^d /submm ^e
SSA22-Sb5-LAB2	22:15:30.27	+00:27:43.6	107	53 ± 7	2.1 ± 0.3	0.66	-0.1	—	—
SSA22-Sb6-LAB4	22:14:09.58	+00:40:54.6	107	32 ± 4	2.0 ± 0.2	0.79	-0.1	3.116 ⁿ	—
SSA22-Sb1-LAB3	22:17:59.14	+00:15:28.7	103	75 ± 9	5.2 ± 0.2	0.48	1.7	3.096 ^o	X-ray ^p
SXDS-N-LAB1	02:18:21.31	+04:42:33.1	101	68 ± 5	3.3 ± 0.2	0.51	-0.4	—	—
SSA22-Sb1-LAB16	22:17:29.01	+00:07:50.2	101	28 ± 8	0.8 ± 0.2	0.80	-0.2	3.104 ^q	X-ray ^r /Spm ^d /submm ^e

^a Major-axis diameter. ^b Filamentarity ($F = 0$ for a circle, $F = 1$ for a filament, see text for more detail). ^c Steidel et al. (2000). ^d This work. ^e Sien et al. (2007). ^f Berger et al. (2002). ^g Matsuda et al. (2005). ^h Matsuda et al. (2005). ⁱ Weib et al. (2009). ^j Chapman et al. (2001). ^k Bass-Zych & Scharf (2004). ^l Condon et al. (1998). ^m Alexander et al. (2003). ⁿ Geach et al. (2005). ^o Geach et al. (2009).

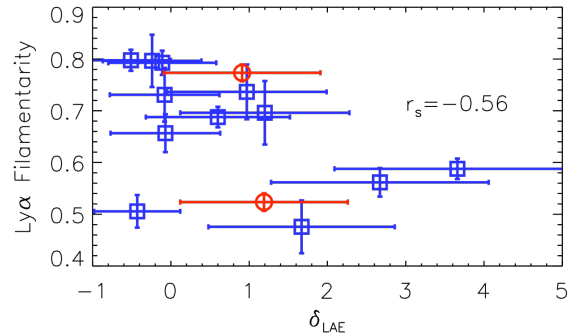


Figure 1. - Filamentarity of the 14 LABs as a function of the overdensity of LAEs. The blue squares and red circles indicate giant LABs without QSO and with QSO, respectively. The error bars show 1σ uncertainties. The filamentarity of the LABs shows a weak anti-correlation with the overdensity of LAEs. The definition of the filamentarity is

$$F \equiv 1 - ((\text{isophotal area}) / (\pi \times (a/2)^2))$$

where a is the major-axis diameter of the LABs. For example, a circle has $F = 0$ and an extremely thin filament has $F = 1$.

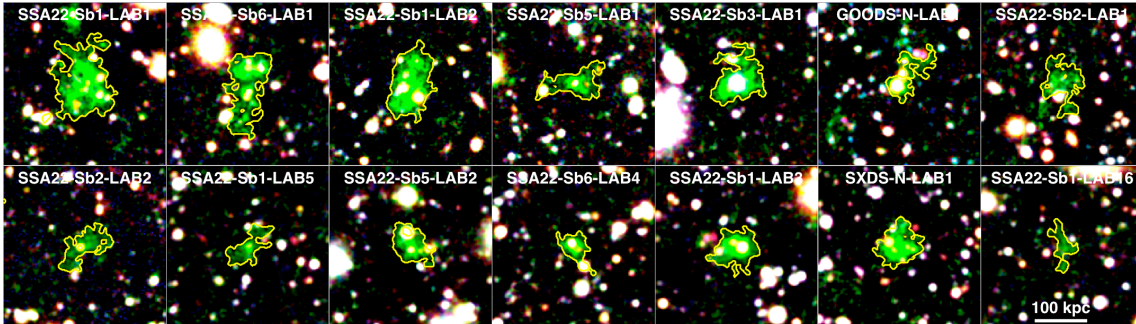


Figure 2. - Pseudo-colour images (B for blue, N B497 for green, V for red) of the 14 giant LABs. The size of the images is 40×40 arcsec² (300×300 kpc²). The yellow contours indicate isophotal apertures with a threshold of 1.4×10^{-18} erg s⁻¹ cm⁻² arcsec⁻². The white horizontal bar in the lower right image represents the angular scale of 100 kpc (physical scale) at z = 3.1.

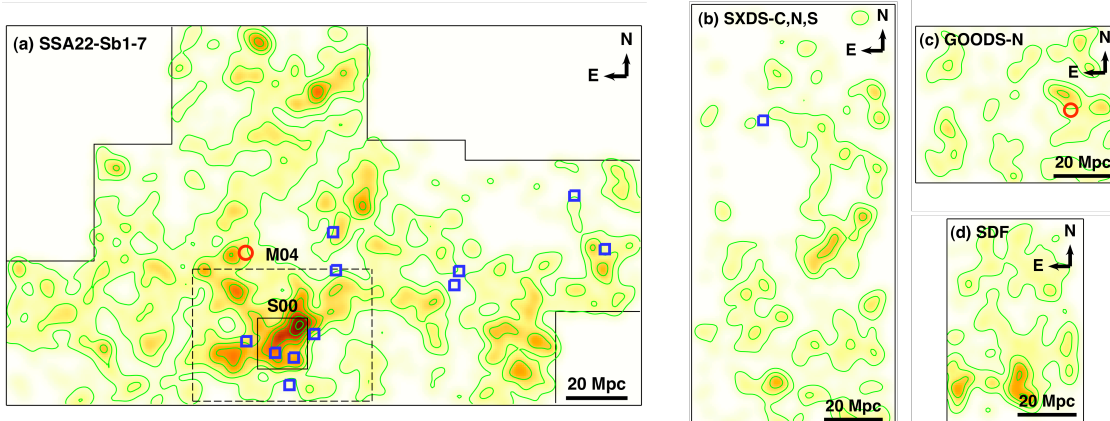


Figure 3. - Sky distribution of the 14 giant LABs and smoothed density maps of ~2000 compact LAEs at z = 3.09. In the left panel (a), the small black box indicates SSA22a field by Steidel et al. (2000, S00) and the dashed box indicates SSA22-Sb1 by Matsuda et al. (2004, M04). The thick bars show the angular scale of 20 comoving Mpc at z = 3.1. The blue squares and red circles indicate the giant LABs without QSO and with QSO, respectively. The contours represent LAE overdensity, $\delta = 0, 1, 2, 3, 4, 5$, and 6.